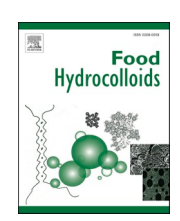
ELSEVIER

Contents lists available at ScienceDirect

Food Hydrocolloids

journal homepage: www.elsevier.com/locate/foodhyd





The influence of lyophilisation on the stability and structural properties of egg yolk granules and prepared emulsion

Beatrice Mofoluwaso Oladimeji ^a, Thomas Pütz ^a, Baohu Wu ^b, Theresia Heiden-Hecht ^b, Olaf Holderer ^b, Stephan Förster ^b, Ronald Gebhardt ^{a,*}

- ^a Chair of Soft Matter Process Engineering (AVT.SMP), RWTH Aachen University, 52074, Aachen, Germany
- b Jülich Centre for Neutron Science (JCNS) at Heinz Maier-Leibnitz-Zentrum (MLZ), Forschungszentrum Jülich GmbH, Lichtenbergstr. 1, 85747, Garching, Germany

ARTICLE INFO

Keywords: Lyophilisation Egg yolk granules Structural characterisation Protein-lipid interaction Emulsion stability

ABSTRACT

Non-lyophilised and lyophilised egg yolk granules (EYG) were analysed using small-angle X-ray scattering. The results showed that the peak at $0.19~\text{\AA}^{-1}$ in the scattering curves disappeared after lyophilisation, indicating the loss of low-density lipoprotein from the granules. At the same time, the Porod slope became steeper, suggesting sharper protein-water interfaces. Enhanced hydration was further confirmed by the higher hydrodynamic radii obtained from dynamic light scattering measurements, which reflect increased water association or swelling of the particles. Additionally, the zeta potential decreased, indicating reduced colloidal stability and increased interfacial activity. The stability of emulsions at 1.5, 3, and 10 % concentrations of both non-lyophilised and lyophilised EYG was investigated using backscattering analysis over 24 h, following testing of a broader range of concentrations. Backscattering stability indices showed that lower concentrations experienced a faster rate of stabilisation change, while higher concentrations demonstrated better stability. Lyophilisation improved stability at higher concentrations, as evidenced by confocal microscopy and SDS-PAGE results. These findings offer insights into the structure-function processing relationships of EYG and their potential applications in emulsions.

1. Introduction

Lyophilisation, also known as freeze-drying, is a gentle drying operation widely used for retaining the quality of biological, food, pharmaceutical and other high-value commercial products. Although the process may be costly in food processing, owing to high energy consumption and high costs of both operation and maintenance (Ciurzyńska & Lenart, 2011) compared to other drying technologies, such as spray drying, and vacuum drying. Spray drying could result in the denaturation of the egg proteins (Vargas-del-Río et al., 2022), disruption and unfolding the spatial structure of egg yolk proteins, protein interactions and aggregate formation (Hu et al., 2023). Thus significantly reducing the emulsification properties of the egg yolk powder compared to fresh egg yolks (Hu et al., 2023). However, lyophilisation is a non-thermal drying technique that promises quality products with acceptable physical, chemical, nutritional, structural and sensory properties (Alcay et al., 2016) after reconstitution. It is considered suitable for protein biomolecules such as egg yolk, providing stable quality and structure (Alcay et al., 2016).

Liquid egg yolks are extensively used in various industries, freezing them facilitates transportation, and extends shelf life, but temperatures below -6 °C could diminish their fluidity and cause gelation, limiting their functionality. In addition, egg yolk in its whole form provides low added value but fractionating it into insoluble protein aggregates (granules) and a clear yellow fluid suspension (plasma) expands its application and increases its value. The egg yolk granule (EYG) component has many interesting characteristics compared to whole egg yolk, including low cholesterol, low fat, high protein, excellent folate (Naderi et al., 2017), high-density lipoproteins (HDL), and other health-benefiting constituents (Oladimeji & Gebhardt, 2023). They range in size from 900 nm-2000 nm, and their components are pseudo-molecular (70 % HDL) and spherical (~14 % LDL) in structure, compactly linked by phosphocalcic bridges to phosvitin (16 %) (Oladimeji & Gebhardt, 2023). In addition to their nutritional profile, egg proteins, including those found in the yolk granules, exhibit excellent emulsifying properties and are being explored increasingly as functional carriers in food and biomedical applications (Tian et al., 2024). EYGs have also been used to create functional materials, such as

E-mail address: ronald.gebhardt@avt.rwth-aachen.de (R. Gebhardt).

^{*} Corresponding author.

antimicrobial edible films (Khan et al., 2025), however, their functionality and stability are sensitive to the treatment applied during the processing. In addition, for ease of handling and storage, interest in dried egg products has increased compared to shelled eggs (Naderi et al., 2017). Heat-drying granules, especially at high temperatures (above 82 °C), have been shown to disintegrate some of the non-lyophilised HDL-phosvitin-complexes, causing a high degree of structural unfolding of proteins and lipoproteins (Thierau et al., 2014). However, freeze-drying granules has allowed for the complete reconstitution of the non-lyophilised structures by rehydration, resulting in structure-related stable granules, due to the high amount of unfreezable water of granules (Thierau et al., 2014). Freeze-drying of egg yolk post-dilution and centrifugation has been reported by Laca et al. (2010) to allow for the separation of the granules, and it has proven to be capable of extending the fraction's shelf life (Oladimeji & Gebhardt, 2023).

Furthermore, zeta potential (surface charge of particles in the system) and hydrodynamic sizes are valuable parameters in measuring the stability of the assembled structure of EYG (Ye et al., 2023) in a dispersion, suspension or emulsion. Zeta potential of egg protein ranges from 0 to -35 mV, depending on the component, method of treatment, product composition, and the final product (X. Li et al., 2021; Shen et al., 2019). In addition, processing techniques such as lyophilisation have a crucial impact on surface charge, particle size and size distribution (Gatto & Najahi-Missaoui, 2023) and have been reported to improve the protein stability in egg white powder (Soraiyay Zafar et al., 2023).

While the intermolecular structure of EYG may be complex, characterisation using advanced microscopy techniques can help identify each component, irrespective of the subjected conditions, without destroying the physiological process and physical structure. Previous studies have demonstrated that the structure of EYG is pH-dependent, with techniques such as atomic force microscopy (AFM) and Grazingincidence small-angle X-ray scattering (GISAXS) revealing changes in LDL incorporation and internal organisation, underscoring the relevance of advanced structural characterisation in assessing the effects of freezedrying (Strixner et al., 2014). Small-angle X-ray scattering (SAXS) has shown that adding water to egg yolk affects the quaternary protein structure, leading to a destabilised lipoprotein dispersion (Gerony et al., 2025). Anthuparambil et al. (2024) demonstrated that structural changes in the egg yolk are linked to an increased disruption of yolk granules and delayed aggregation of low-density lipoproteins (LDL), due to an increase in the concentration of NaCl. The authors reported that at $q\sim0.02~\text{Å}^{-1}$, the SAXS curves showed LDL vesicles with a diameter of approximately 30 nm. When the LDL vesicles aggregate, the peak shifts to lower q values, indicating larger structures and aggregation. An aggregation shift was also observed in LDL gelation following a temperature increase (Anthuparambil et al., 2023). These salt-induced restructurings lead to a decrease in the Porod slope and improved solubility of the protein components, indicating a transformation of the colloidal microstructure of the egg yolk. Although SAXS and Ultra-SAXS techniques have been explored to differentiate components of whole eggs and heated egg yolk (Anthuparambil et al., 2023; Oka et al., 2022), none of these previous methods have combined the use of SAXS to understand EYG, especially those free of solvents, salt and other chemical additions, or compared the effect of freeze-drying. This study will provide detailed insight into the stability, structure, and components of EYG.

Additionally, egg yolks in their natural form are widely used to prepare food emulsions due to their high contents of amphiphilic proteins; however, their poor solubility is disadvantageous to their emulsifying property, making it problematic to play a full role at the emulsion interface (Bie et al., 2025). On the other hand, the composition, sizes, and structure of EYG allow them to act as natural emulsifiers and stabilisers in oil-in-water emulsions. Research has shown that EYG are stabilising and nutritional emulsifying ingredients in several food products, such as mayonnaise (Motta-Romero et al., 2017), infant formula, salad dressing, baked products, etc, and they have demonstrated

superior emulsion stability compared to whole volk and plasma (Suhag, 2024). No noticeable rheological differences were reported between low-fat mayonnaise prepared using freeze-dried and fresh EYG (Suhag, 2024). This signifies that lyophilised EYG will offer a promising alternative to fresh eggs and components, as they are preserved supramolecular structure capable of forming protein-lipid interfacial films in emulsion, encapsulation and functional food formulations. Also, emulsions stabilised with bio-based particles such as lyophilised EYG are alternatives to addressing environmental challenges. This study aims to prepare a storable dehydrated EYG that can retain its functionality after freeze-drying, and to investigate the structure-function relationships of the lyophilised and non-lyophilised EYG. It will give information on zeta potential, hydrodynamic sizes, internal structure, and emulsion stability. Results from this study will help to understand the functionality of EYG protein particles in emulsions and other functional applications, to serve as an alternative to whole eggs, egg yolks, other surfactants and nanoparticles; and a sustainable, clean-label ingredient for food product development.

2. Materials and methods

2.1. Materials

Fresh brown eggs and rapeseed oil were purchased from a supermarket in Aachen, Germany. They were transported to the laboratory, where the EYG were prepared the same day. All reagents were of analytical grade from Sigma Aldrich, USA.

2.2. Preparation of the EYG

The EYG were prepared using the modified Li et al. (2021) method. Eggs were manually broken, and the yolk was separated from the albumen. The chalazae were carefully removed using tweezers, and the residual egg white was removed by rolling the yolk on particle-free blotting paper. The vitelline membrane was pierced to drain the yolk into a beaker, the yolk was diluted with the same volume of Milli-Q water, stirred, and then centrifuged at 10,000 g (Universal 320 R, Germany) at 4 $^{\circ}C$ for 45 min. The precipitates were collected as the sediment arising from centrifugation, washed twice by resuspending them in twice their volume in Milli-Q water at 4 $^{\circ}C$ for 1 h, stirred gently (for 1 h in the refrigerator at 4 $^{\circ}C$), and centrifuged (10,000 g for 45 min at 4 $^{\circ}C$). The supernatant was removed, and the granule was collected.

2.3. Lyophilisation processing of the EYG

A portion of the freshly fractionated EYG was frozen in liquid nitrogen (N2) for 3–5 min to become solid. Each sample was contained in a vial, placed on the freeze-dryer (Christ Alpha 1–4 LO plus, Germany) and freeze-dried under vacuum conditions for approximately 72 h.

2.4. Preparation of lyophilised and non-lyophilised EYG emulsions

A simple emulsion system was used as a model to assess the ability of the lyophilised and non-lyophilised EYG to adsorb to oil-water interfaces and contribute to droplet stabilisation. Before the preparation, the moisture content of each EYG was determined using a moisture analyser (Sartorius MA 37, Germany), and the granule was diluted in ultrapure water (filtered through the Ultrapure water system simplicity, UV, Merck, Germany). About 9.5 g of the EYG dispersion was measured into a beaker, 9.5 g of the rapeseed oil was measured into the dispersion, and mixed with a high-performance dispersing instrument (Ultra Turrax, IKA T25, Germany) at 12,000 rpm (and 20,000 rpm in the case of droplet size measurement) for 1 min (Q. Li et al., 2020; Mi et al., 2022; Wang et al., 2020). The freshly prepared emulsions were immediately filled into the vials for further measurements. Thermodynamically, a rough logarithmic scale would have been 1.5, 3, and 6 %, but 10 % was

selected as the upper limit instead of 6 % because that was where the greatest effect occurred during the preliminary study. Therefore, final concentrations of 1.5 %, 3 % and 10 % EYG in each emulsion were prepared for this study.

2.5. Methodology

The following analyses were carried out on all the EYG samples for stability and microstructural determination.

2.5.1. Structural analysis of the EYG (SAXS measurement)

Before the Small-angle X-ray scattering (SAXS) measurement, the non-lyophilised and lyophilised EYG were prepared by redispersing each sample in ultrapure water. Both dispersions were gently stirred (for 1 h at 60 rpm) to ensure a homogeneous mixture, and the structural integrity of the granules remained intact. The final concentration of the freeze-dried granule was 25.9 % w/w, while that of the non-lyophilised sample was determined from it, based on the correction factor applied to the SAXS curves.

The experiments were conducted using the laboratory-based SAXS-WAXS beamline, KWS-X (XENOCS XUESS 3.0 XL, France), at JCNS-MLZ in Garching, Germany, according to the method described by Heiden-Hecht et al. (2024). The MetalJet X-ray source (Excillum D2+) was operated at 70 kV and 3.57 mA, emitting Ga-Kα radiation with a wavelength of $\lambda = 1.314$ Å. The sample-to-detector distances ranged from 0.5 m to 1.70 m, covering the scattering vector Q range from 0.003 to 1.2 Å⁻¹ [Q is the scattering vector: where $Q = (4\pi/\lambda) \sin(\theta)$, and 2θ represents the scattering angle]. Sample measurements were performed at room temperature (25 $^{\circ}C$) in sealed glass capillaries with a diameter of 2 mm. The SAXS patterns were normalised to the absolute scale and azimuthally averaged to obtain intensity profiles, with the background subtraction using empty capillary data. The Porod slope was determined by non-linear fitting of the function $I(q) = k \cdot q^{-n}$ in the q range of 3. $10^{-3} - 7.10^{-3} \text{ Å}^{-1}$. This yielded a high coefficient of determination (R² = 0.9957) and corresponds approximately to the region used in a previous study (Anthuparambil et al., 2024). To determine the mean scattering vector and peak width in the range $q = 1.10^{-2} - 1.10^{-1} \text{ Å}^{-1}$, two Gaussian profiles were fitted to the non-lyophilised sample, while one Gaussian function combined with a power law was used for the lyophilised sample. Non-linear fitting was performed, yielding coefficients of determination of $R^2 = 0.992$ for the non-lyophilised sample and $R^2 = 0.999$ for the lyophilised sample. Independent biological duplicate samples were prepared for analysis, and the SigmaPlot was employed for data presentation and using non-linear fitting analysis.

2.5.2. Stability (DLS) measurement of the EYG

The hydrodynamic diameter (Dh) and zeta (ζ) potential values of lyophilised and non-lyophilised EYG were measured to determine the stability of the granules. Before measurement, the concentration of each sample was adjusted to 1 mg/ml by re-dispersing in Milli-Q water (Ye et al., 2023). The ζ -potential of the diluted granule dispersions was determined in the standard folded capillary electrophoresis cells using the Zeta analyser (Zetasizer Lab, ZSU3100, Malvern, UK). All the measurements were conducted at 25 $^{\circ}C$ after the samples were incubated for 2 min for temperature equilibrium. Each zeta-potential data point was reported as the average and standard deviation of at least three reported readings made on independent biological triplicate samples (X. Li et al., 2021; Mi et al., 2022). The average particle size distribution (Dh) value of the EYG suspension was determined in the cuvettes using the same system.

2.5.3. Microscopic evaluation of the emulsion samples

After emulsion preparation in independent biological replicates, 200 μ L of each emulsion was immediately transferred onto a glass slide, and several images at different positions were taken using a microscope

(VHX 7000, Keyence, Germany) with $100\times$ magnification. The droplets were automatically detected using the Hough Circles function from the OpenCV package for Python, and their size was measured. All emulsions were measured in technical triplicate.

2.5.4. Time-dependent stability study of the emulsion samples

The stability of the emulsion was measured using a Multiscan MS 20 (DataPhysics, Instruments GmbH, Filderstadt, Germany) according to the modified method described by Sztorch et al. (2023). A small vial filled with the freshly prepared emulsion sample was placed in the instrument's scan towers and scanned every 30 min for 24 h at 25 °C. The measured zone was between 0 mm (bottom of the glass) and 45–50 mm (fill level of the glass). The transmission and backscattering intensity were measured, and the stability of each emulsion was derived from the detected signal.

2.5.5. Confocal scanning of the most stable EYG emulsion concentrations

Imaging was performed on the most stable non-lyophilised and lyophilised emulsions using an LSM 980 Airyscan 2 confocal laser scanning microscope (Carl Zeiss Microscopy GmbH, Germany). Before the scanning, the emulsions were prepared by dissolving each EYG in Milli-Q water with 1 g of a 1 mM rhodamine B solution (Sigma Aldrich, USA) to achieve a final EYG concentration of 10 % (w/w). The mixture was stirred overnight, and excess dye was removed by washing the solution twice (centrifugation at $10,000 \times g$ for 45 min at 4 °C) each time, followed by resuspension of the pellet in Milli-Q water. The emulsion was then prepared as previously described. Before confocal imaging, the emulsion was diluted 1:50 in Milli-Q water. Fluorescence excitation was performed at 546 nm, and emission was detected at 567 nm.

2.5.6. SDS-PAGE analysis of the most stable EYG emulsion samples

After the non-lyophilised and lyophilised EYG emulsion samples (10 % concentration) were prepared, they were allowed to stand at room temperature for 30 min for protein adsorption. The interfacial proteins were recovered by centrifuging the emulsions gently at 3000 $x\,g$ for 30 min at 4 $^{\circ}C$, and the upper (cream), middle and lower layers were collected separately.

The protein of these samples and that of the whole non-lyophilised and lyophilised EYG were extracted by diluting (1:1, v/v) with deionised water to reduce viscosity and facilitate homogenisation. Aliquots of 100 µL from this suspension were mixed with five volumes of ice-cold acetone containing 10 % (w/v) trichloroacetic acid (TCA) and incubated for 60 min at -20 °C. Samples were centrifuged at 15,000 x g for 15 min at 4 °C, and the supernatant was discarded. The resulting protein pellets were washed twice with 100 % ice-cold acetone (-20 °C, 5 min each) followed by centrifugation (15,000 x g, 5 min, 4 $^{\circ}C$). After brief air-drying, pellets were solubilised in 200 μL of solubilization buffer containing 8 M urea, 2 % SDS, 50 mM Tris-HCl (pH 8.0), and 10 mM dithiothreitol (DTT) at 70 °C for 15 min. Insoluble material was removed by centrifugation (15,000 x g, 5 min, 4 $^{\circ}C$), and the supernatants were collected for subsequent analysis. Protein concentration was determined using the Bradford assay. Due to high detergent concentrations in the solubilization buffer, samples were diluted 40-fold to reduce background interference.

For SDS-PAGE analysis, protein extracts were mixed 1:1 with SDS sample buffer [50 mM Tris-HCl, pH 6.8, 10 % glycerol, 4 % (w/v) SDS, 2 % (v/v) β -mercaptoethanol, and 0.03 % (w/v) bromophenol blue]. A total of 15 μg protein was loaded per well on NuPAGETM 4–12 % Bis-Tris gels (1.0 mm, 15 wells; Thermo Scientific) using 20 \times MES running buffer (1 M MES, 1 M Tris, 2 % SDS, 20 mM EDTA, pH 7.2) diluted 1:20 in deionised water. Approximately 2 μL of PageRulerTM Prestained Protein Ladder (10–180 kDa; Thermo Scientific) was loaded as a molecular weight standard. Electrophoresis was performed at 100 V for 10 min followed by 200 V for 80 min. After electrophoresis, gels were stained overnight with Coomassie Brilliant Blue R-250 staining solution [10 % (w/v) ammonium sulfate, 1.2 % (v/v) phosphoric acid (85 %),

0.1 % (w/v) Coomassie Brilliant Blue R-250, supplemented with 20 % (v/v) methanol] before use. Excess dye was removed by destaining with deionised water.

2.5.7. Statistical analysis

All samples were prepared in independent biological triplicate, experiments were performed in technical triplicate and expressed as the mean \pm standard deviation. Data analysis and visualisation were presented using Origin statistical software (2023). The mean comparisons were analysed using one-way, two-way ANOVA, and the Tukey test for post hoc comparisons.

3. Results and discussion

3.1. Nano-structural characterisation of the EYG by SAXS

The prepared non-lyophilised and lyophilised EYG dispersions were analysed using SAXS, and the scattering functions per unit sample path length (cm $^{-1}$) are presented in Fig. 1. To allow a clear comparison of the structural features, the SAXS curve of the lyophilised sample, which has a higher scattering intensity due to its higher concentration, was multiplied by a factor of 0.61 to normalise the intensity at the highest q values. Based on this correction factor and the known concentration of the lyophilised sample (25.9 % w/w), the granule concentration in the non-lyophilised dispersion was estimated to be approximately 15.8 % (w/w), assuming a linear scaling of SAXS intensity with particle concentration.

To check for possible concentration effects, we measured diluted EYG samples. In both lyophilised and non-lyophilised cases, the diluted curves lie below the respective undiluted curves shown in the supplementary document (Fig. S1). The diluted lyophilised sample also lies below the undiluted non-lyophilised sample, reflecting its lower effective concentration. However, the characteristic SAXS features (shoulders, minima, and the Porod range), and accordingly the corresponding structural properties on length scales of $\sim\!1\!-\!100$ nm, remain unchanged within the investigated concentration range and are therefore not sensitive to concentration variations.

The SAXS curves of non-lyophilised and lyophilised granular

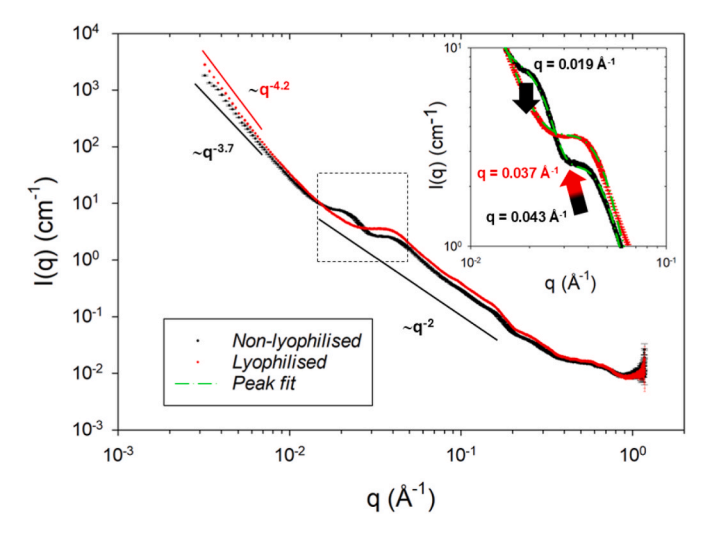


Fig. 1. Log-log plot of the SAXS intensity as a function of the scattering vector q for the non-lyophilised (black dots) and lyophilised (red dots) egg yolk granules.

The intensity is shown on an absolute scale in cm-¹, corresponding to the differential scattering cross section per unit length of the sample. The inset highlights the mid-q region with two distinct peaks. The green dashed lines represent the Gaussian fits used to determine the peak positions and widths. Variations in the shape and position of the peaks reflect structural changes caused by the lyophilisation process.

dispersions cover a scattering vector range from q=0.003 to $1.2\ \text{Å}^{-1}$. In the low q region (q = 0.003–0.01 Å $^{-1}$), the lyophilised sample shows a significantly higher scattering intensity compared to the non-lyophilised sample. In this region, both samples follow a power-law behaviour; the non-lyophilised granules show a slope of q $^{-3.7}$, while the lyophilised granules follow a much flatter decay with a slope of q $^{-4.2}$. The higher intensity and lower exponent observed for the lyophilised granules suggest that the overall granule structure has expanded and the particle surfaces have become smoother after lyophilisation and redispersion.

In the intermediate q range (q = $0.01-0.2 \text{ Å}^{-1}$), a q⁻² power-law decay is observed, which, according to scattering theory, is characteristic of random coil-like polymer structures (Heiden-Hecht et al., 2024). A q⁻² decay has also recently been observed in whole egg yolk preparations within this q-range (Gerony et al., 2025). However, as our results suggest, this scattering behaviour is more likely to be characteristic of the granule-associated HDL structure, a major structural component of egg yolk. The distinctive peak associated with HDL, which is found at q = 0.037 Å^{-1} in the non-lyophilised sample and indicates internal structural features, shifts towards lower q values after lyophilisation. This is consistent with an expansion of the HDL structure. Notably, the q⁻² decay region in the lyophilised sample exhibits increased scattering intensity compared to the non-lyophilised sample, corresponding with a parallel upward shift in the log-log plot. This increase is due to the expansion of the random coil-like HDL structures, causing them to become larger and scatter more X-rays. It is also due to the loss of LDL domains, enhancing the electron density contrast between HDL and the surrounding matrix.

Additionally, in the intermediate q range (q = 0.01– $0.1~\text{Å}^{-1}$), two distinct peaks are visible in the non-lyophilised sample. Peak fitting yielded characteristic positions at q = $0.019~\text{Å}^{-1}$ and q = $0.037~\text{Å}^{-1}$, as shown in the inset of Fig. 1. Both peaks had been detected in previous studies on egg yolk samples, with the first peak attributed to LDL (Anthuparambil et al., 2024). A Gaussian fit to the first peak gave a full width at half maximum (FWHM) of $0.0052~\text{Å}^{-1}$, indicating a relatively narrow size distribution of LDL domains. However, the absence of higher-order maxima suggests that the LDL are randomly distributed within the granules rather than forming ordered arrays.

Notably, the first peak disappears completely in the lyophilised sample, strongly suggesting that LDL are released from the granule structure during lyophilisation. This interpretation is further supported by the observed phase separation and visible creaming upon rehydration of the lyophilised powder, where surfactant material probably derived from released LDL, accumulated at the liquid-air interface. The second peak remains visible in the lyophilised sample but is shifted to a lower q (from 0.037 to 0.031 Å^{-1}), indicating a larger real-space distance. We attribute this feature to the internal structure of HDL and interpret the shift as a result of internal expansion, probably caused by the removal of LDL during lyophilisation. These SAXS results show that lyophilisation alters the internal structure of the granules, primarily through the loss of LDL, resulting in a more expanded and smoother internal architecture. The presence and shift of structural peaks further indicate that the LDL and HDL domains respond differently to lyophilisation. To further investigate how these structural changes affect the colloidal properties of the granules, dynamic light scattering (DLS) was performed to assess changes in overall particle size and zeta potential measurements were performed to evaluate surface charge and colloidal stability of the dispersions.

3.2. Zeta potential and hydrodynamic size measurement of the EYG

The EYG fractionated from fresh eggs were prepared for dynamic light scattering analysis by diluting them in Milli-Q water (1 mg/ml) to ensure optimal particle dispersion during measurement. The hydrodynamic size, polydispersity index (PDI), and zeta potential data were obtained from the Zetasizer instrument. At the time of measurement, the pH of the lyophilised EYG was 6.50 \pm 0.51, and that of the non-

Food Hydrocolloids 172 (2026) 112170

lyophilised EYG was 6.90 ± 0.08 .

The zeta potentials of the lyophilised and non-lyophilised EYG particles were plotted against their hydrodynamic sizes (Fig. 2). The mean (\pm SD) values are -16.60 ± 0.69 mV and -18.87 ± 0.90 mV for the lyophilised and non-lyophilised EYG, respectively. While the zeta potential values of both EYG samples are within the range (-16 to -30mV) classified as having incipient instability behaviour, the nonlyophilised samples demonstrated slightly higher zeta potential compared to the lyophilised ones, with statistically significant differences ($P \le 0.05$). These differences may be attributed to the combined effects of lyophilisation (change in surface charge characteristics) and dilution effect (modified ionic environment, pH, surface charge, particle dispersion and interactions) between the two granule samples (Fernandez-Moure et al., 2018; Malvern, 2010). Additionally, the less negative zeta potential values in lyophilised EYG suggest that some of the charged groups may have been buried within the aggregates formed during the drying and reconstitution process, thereby reducing their contribution to electrostatic repulsion. The zeta potential values obtained in this study are lower than those reported for natural EYG (-20mV), and EYG at pH 7 (-20.46 ± 0.50 mV) (X. Li et al., 2021; Shen et al., 2019), but higher than those (-16.23 \pm 0.39 mV) reported for high-pressure homogenised EYG (Liu et al., 2024). The differences may be due to their different processing/treatment, pH, sources, and egg components. The low negative zeta potential values from this result indicate that particles in this suspension have little or no force to prevent them from coming together and flocculating; thus, the suspension may aggregate under stress.

The results of the hydrodynamic sizes are 1142.89 \pm 50.76 nm and 967.9 ± 103.27 nm for the lyophilised and non-lyophilised EYG, respectively, as shown in Fig. 1. The values obtained in this study are higher than those reported (605.23 \pm 10.73 nm) for high-pressure homogenised EYG (Liu et al., 2024), while the non-lyophilised sample value is similar to that reported for untreated chicken egg yolk (900.20 \pm 45.09 nm) granule (Zhang et al., 2025). The variations in the hydrodynamic sizes of the different EYG suspensions may be due to the differences in the dispersion stability, the composition of the high-density lipoproteins (HDL), low-density lipoproteins (LDL), and phospholipids of each EYG, or even differences in the sample preparations. In addition, the lyophilised samples are significantly (P < 0.05)larger than the non-lyophilised ones. This may be due to the aggregation induced during the process of freeze-drying, structural changes of the protein and lipids during the drying process, or even the clustering of particles upon rehydration. However, SAXS measurements do not reveal the formation of new scattering features or additional structural motifs in the low-q or mid-q range, which would typically accompany such phenomena. Therefore, extensive aggregation appears less likely. Instead, the observed size increase is more plausibly attributed to the expansion of the remaining HDL structures within the granules. As

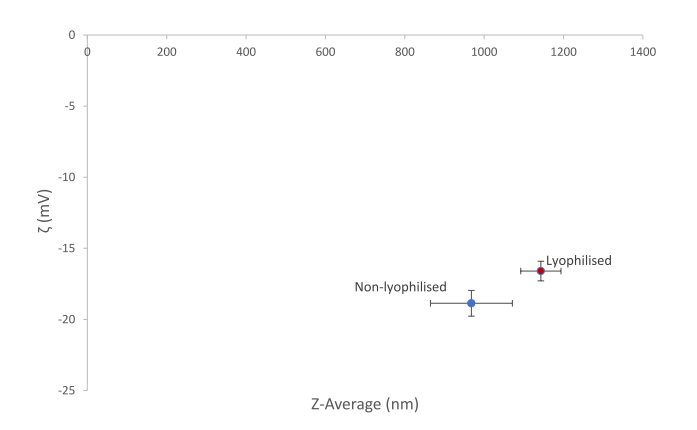


Fig. 2. Zeta potential vs hydrodynamic size of the egg yolk granules.

described in the previous chapter, small-angle X-ray scattering (SAXS) shows that the LDL-associated peak ($q=0.019~\mbox{Å}^{-1}$) disappears upon lyophilisation, suggesting that the LDL components are displaced from the granule. At the same time, the HDL-associated peak shifts from $q=0.037~\mbox{Å}^{-1}$ to $q=0.031~\mbox{Å}^{-1}$, which corresponds to an increase in structural spacing of around 20 %. This strongly suggests that the HDL architecture has expanded. This expansion could account for the increase in hydrodynamic size observed using DLS, as the remaining HDL becomes more hydrated and occupies a larger effective volume. In line with this, the standard deviation of the particle size distribution decreases after lyophilisation, suggesting that the particles are more uniform in size and shape. This is likely due to the formation of rounder, more defined HDL-based structures.

The freeze-drying process can significantly impact the surface charge and size distribution of EYG. High-density lipoproteins (HDL) contribute a substantial negative zeta potential to non-lyophilised EYG due to their hydrophilic properties. However, during lyophilisation, water removal has caused a significant alteration in the lipoprotein component of the egg yolk. Although the lyophilised EYG was rehydrated before DLS measurement, the relative LDL concentration remains unchanged, potentially limiting its surface-active properties if rehydration is incomplete or uneven, and the influence of HDL may also be diminished. Consequently, lowering the overall negative surface charge of the lyophilised suspension, reducing the zeta potential and thus the electrostatic stability of the suspension. Additionally, lyophilisation can lead to changes in pH and ionic strength (Bhosale et al., 2021), which may destabilise protein structure, including the LDL, making the granules more prone to water absorption and expansion.

Likewise, the polydispersity index (PDI) result from the measurement revealed that lyophilised samples have statistically ($P \leq 0.05$) higher PDI values (0.66 \pm 0.34 and 0.73 \pm 0.40) than their nonlyophilised counterparts (0.30 \pm 0.25 and 0.29 \pm 0.18). The values obtained for EYG in its natural state are similar to those reported (0.29

 \pm 0.01; 0.47 \pm 0.02) in the literature (Liu et al., 2024; Shen et al., 2019). The PDI value obtained for the lyophilised EYG is greater than 0.7, corresponding to a broader size distribution, indicating their polydispersity (Danaei et al., 2018), while a lower PDI value in non-lyophilised samples affirms their homogeneity. A small PDI (below 0.5) indicates uniformity (Danaei et al., 2018) and values lower than 0.25 indicate better stability. However, rather than resulting from extensive aggregation, which is not supported by SAXS, this increase in PDI is more likely to be due to the presence of both expanded HDL structures and smaller residual components, such as protein fragments or partially reorganised particles. While these may not significantly affect the average hydrodynamic size or scattering features, they do broaden the overall size distribution. This suggests that lyophilisation leads to the formation of larger, more defined structures with a narrower core size distribution while introducing peripheral heterogeneity that increases the PDI.

3.3. Egg yolk granule (EYG) application in emulsion

The application of the fractionated EYG (both lyophilised and non-lyophilised) was investigated in prepared emulsions. A preliminary study of emulsions made from the lyophilised EYG at varying concentration ranges (0.2–10 % EYG, 5–85 % rapeseed oil, and 14–94 % ultrapure water) were carried out to understand their physical behaviour at different decomposition times, as illustrated using a ternary plot (Fig. 3). Each point of the triangle shows the relative proportions of the three components (water, rapeseed oil, and EYG, w/w). The lines indicate the time after preparation at which a phase separation of the emulsion was visible. This corresponds approximately to the stability period of the respective emulsions. Generally, the stability period of the emulsions increases with increasing egg yolk content.

While an emulsion with 35 % (w/w) rapeseed oil and 1 % (w/w) EYG

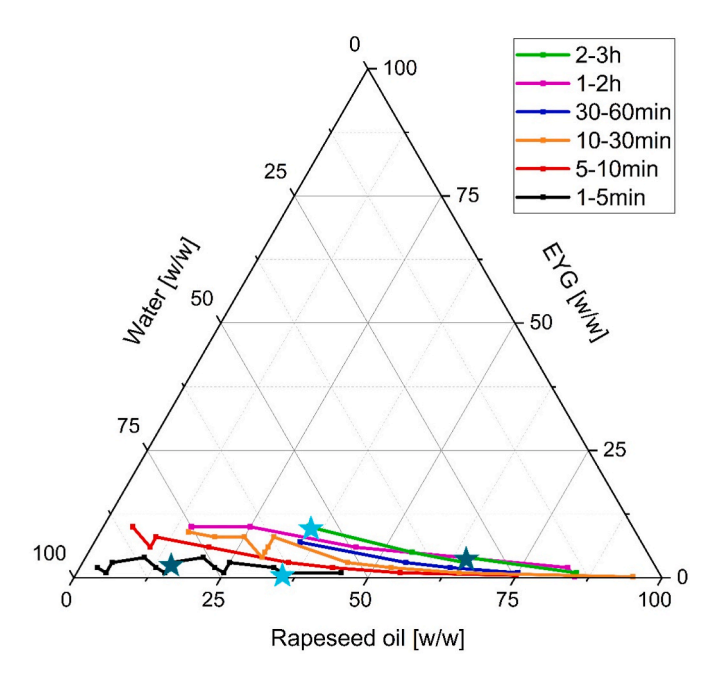


Fig. 3. Ternary plot of emulsions with varying concentrations of water, oil and egg yolk granules.

was only stable for a maximum of 5 min, the emulsion with the same oil content but 10 % (w/w) EYG remained stable for up to 3 h (marked with cyan stars in Fig. 3). Furthermore, stability decreases with increasing water content at the same egg yolk concentration. While the emulsion with 3 % (w/w) EYG and 32 % (w/w) water remained stable for up to 3 h, phase separation was observed after only 5 min at the most with a composition of 3 % (w/w) EYG and 82 % (w/w) water (marked with dark green stars in Fig. 3). A shift towards higher oil and EYG contents (especially near equal ratio) at later timepoints indicates a better incorporation of the oil into the emulsion, and the role of the EYG as stabiliser or structuring agent. This means that an increase in the concentration of the EYG helps to stabilise the oil droplet in the water, indicating a long-term stable emulsion. This preliminary study further suggests the need for a deeper insight into the time-based progression and droplet size of the emulsion, through multiple light scattering and microscopic evaluation.

3.4. Microscopic evaluation of the emulsion samples

Aside from the role of the emulsifier concentration in emulsion preparation, homogenisation creates droplets, and the shear forces applied during this unit operation affect the droplet size distribution, which in turn affects the physical stability of an emulsion (Zanatta et al., 2017). Inadequate or extreme shear energy can influence the stability of the emulsion prepared (Chen et al., 2023). For this aspect of the study, two speeds were selected when creating the emulsion, based on the operating ranges of laboratory-scale rotor-stator homogenisers (such as Ultra-Turrax), a low speed (12,000 rpm, producing moderate shear) and a high speed (20,000 rpm, producing high shear). The microscopic images of each emulsion are presented in the supplementary file (Fig. S2).

The microscopic images revealed the distinct differences in the structure of each emulsion and variations in the droplet sizes of each emulsion, suggesting a polydisperse system, where some droplets coalesced into larger structures, and some remained small. Droplets appear spherical across all conditions, and emulsions made with lyophilised EYG appear slightly larger and less uniform than the non-lyophilised EYG emulsions, except at 10 % granule concentration. Increasing the homogenisation speed from 12,000 rpm to 20,000 rpm resulted in smaller and more densely packed droplets for both the non-lyophilised

and the lyophilised samples. Increasing the EYG concentration (1.5 %-10 %) resulted in a lower droplet density and more uniform sizes for both lyophilised and non-lyophilised EYG emulsions. The role of lyophilisation becomes less noticeable at higher concentrations (10 % EYG), highlighting that both the lyophilised and non-lyophilised EYG at high concentration (10 %) are applicable in emulsions. Further quantitative analysis of the droplet sizes using the Hough Circles function from the OpenCV package for the Python script was done automatically, as illustrated in the supplementary file (Fig. S3). The distribution graph was used to support these visual pieces of evidence (Fig. 4). The mean values (in terms of radius) for each emulsion droplet are presented in Table 1a. They are significantly different at the 0.05 level, except for those prepared using 1.5 % lyophilised EYG. Non-lyophilised EYG emulsions show smaller droplet sizes (8.549 \pm 4.495 μm to 19.242 \pm 9.814 µm) compared to the lyophilised (7.076 \pm 3.319 µm to 23.689 \pm 13.568 µm) counterpart across all emulsions analysed. Lyophilisation increased droplet sizes in 1.5 and 3 % emulsion samples, possibly because the water removal during freeze-drying can cause particles to come into closer contact and form larger aggregates. However, at 10 % concentration, the droplet sizes reduced slightly with lyophilisation, likely because higher concentrations of solids exhibit reduced aggregation due to increased steric stabilisation and decreased mobility of particles (McClements, 2004).

The distribution graph generated using the emulsion's droplet sizes (Fig. 4) revealed that the lyophilised sample had a higher frequency of larger size ranges (>30 μm), indicating a broader distribution across all samples (except at 10 % concentration). This is similar to the report that emulsions made from frozen and subsequently thawed EYG have larger particles (Gmach et al., 2022). Increasing the energy input yielded a slight change (not significant) in the mean droplet size (Table 1a) but rather a narrower distribution width (Fig. 4), indicating more uniform droplet sizes. Furthermore, increasing the emulsifier content yielded more uniform, smaller droplets, which led to a narrower size distribution, likely due to more available emulsifier covering the surface. Emulsion droplets are more homogeneously distributed across the 10 % lyophilised and non-lyophilised samples. This is similar to the report of Mi et al. (2022) an increase in the concentration of EYG promoted a decrease in the droplet particle sizes. The three percentiles of the droplet size distribution for all emulsions varied from 3.79 to 10.61 µm, $6.31-21.72 \mu m$, and $11.11-41.67 \mu m$, corresponding to the D10, D50, and D90, respectively, as shown in Table 1b. Although the droplet sizes of the emulsion samples exceeded a micrometre and might not be considered an ultrafine or highly stable emulsion. The result demonstrates the functional capacity of the lyophilised EYG to form and stabilise emulsion, despite undergoing structural rearrangement during lyophilisation. This highlights their potential utility in real-world food applications. Emulsions stabilised with high-density lipoprotein (HDL) have larger droplet sizes compared to the low-density lipoprotein (LDL)-stabilised ones (Bie et al., 2025). Due to the sizes of HDL particles, they have a lower stacking efficiency at the interface, ultimately resulting in larger droplets. This is why LDL (mainly found in the plasma fraction) holds a higher emulsion capacity than HDL (mainly found in the granular fraction), as a small LDL micelle adsorbs faster at oil-water interfaces than the larger granule particles. While in our study, the plasma fraction high in LDL was removed entirely, report has it that about 12-14 % of LDL is residual in the granule fraction (Abeyrathne et al., 2022; Oladimeji & Gebhardt, 2023), and this seems sufficient to enhance emulsification. Further reduction or removal of LDL in the EYG as a result of lyophilisation may also be responsible for larger droplet sizes in lyophilised EYG emulsions, which is consistent with the findings of Bie et al. (2025) and Gmach et al. (2022). Overall, lyophilisation produced uniform emulsion droplets due to enhanced surface activity of the granules, since the lyophilised EYG can form stable interfaces at the oil-water boundary during emulsification. Increasing the EYG concentration provided more emulsifier to the emulsion but showed droplet crowding. Also, increasing the homogenisation speed breaks down

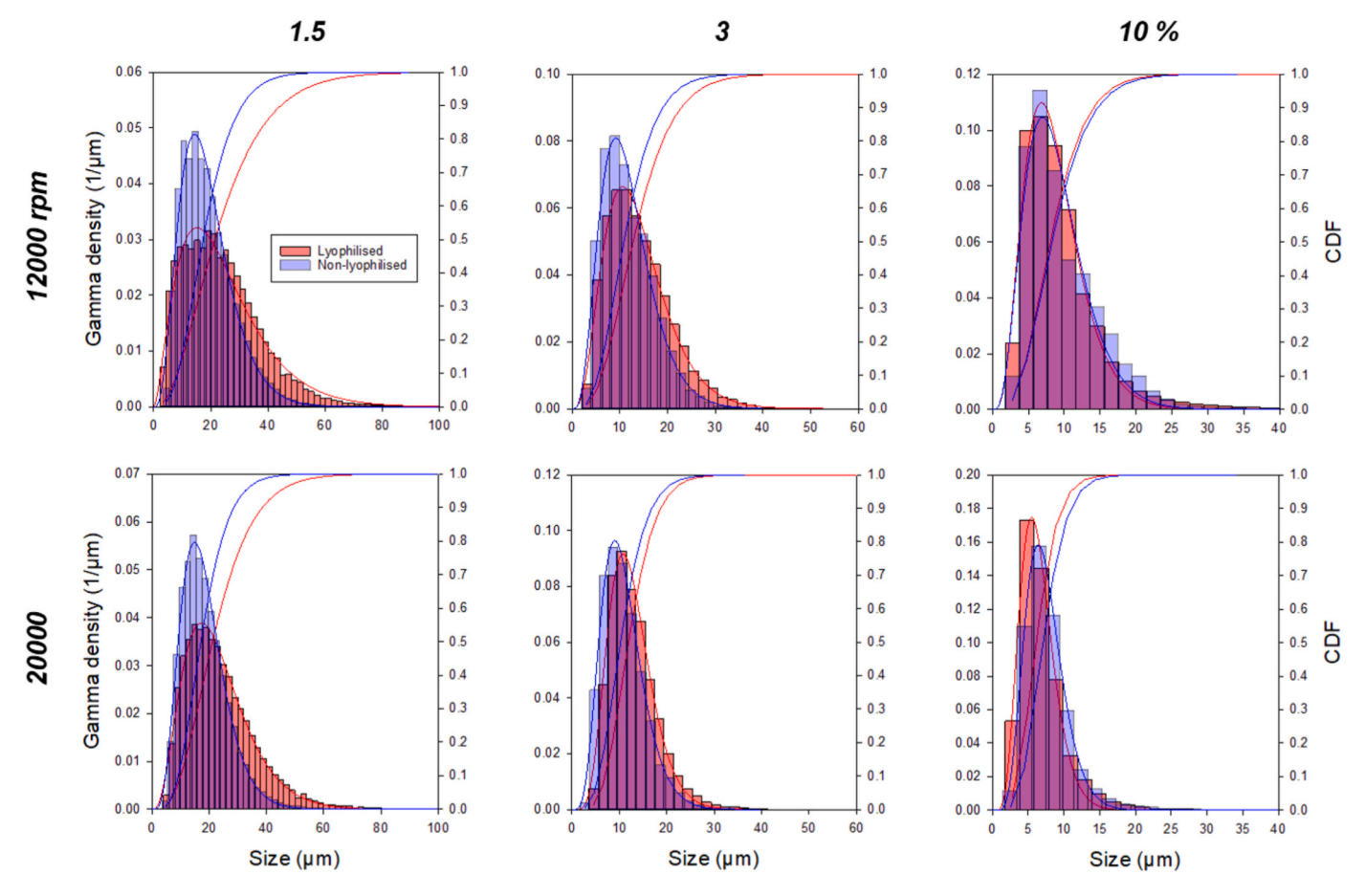


Fig. 4. Droplet size distribution of the non-lyophilised and lyophilised emulsion prepared at varying egg yolk granule concentration and homogenisation speed.

 Table 1a

 Mean droplet sizes of emulsions produced at different EYG concentrations and shear rates.

Shear rates (rpm)	EYG concentration	Non-Lyophilised (μm)	Lyophilised (µm)	
12,000 (rpm)				
	1.5 %	$19.242 \pm 9.814^{\rm b}$	23.689 ± 13.568^a	
	3 %	$11.891 \pm 5.356^{\rm f}$	$14.082 \pm 6.495^{\rm d}$	
	10 %	9.879 ± 5.038^{h}	9.506 ± 5.395^{i}	
20,000 (rpm)				
	1.5 %	$18.673 \pm 8.702^{\rm c}$	23.778 ± 12.330^a	
	3 %	11.050 ± 4.544^{g}	$12.959 \pm 5.290^{\mathrm{e}}$	
	10 %	$7.881\pm3.733^{\rm j}$	7.076 ± 3.319^k	

Means that do not share a letter in the table are significantly different ($P \le 0.05$)

droplets more effectively, which requires more energy input, thus reducing processing efficiency, and excessive shearing could lead to coalescence, especially when emulsifier coverage is inadequate.

$3.5. \ \ \textit{Time-dependent stability study of the emulsion samples}$

Increasing the homogenisation rate generally improves emulsion stability by reducing droplet sizes. Still, practical drawbacks such as increased energy costs, coalescence formation and other emulsion destabilising mechanisms may diminish their functionality. High shear could also increase the risk of air incorporation, which may affect measurements such as backscattering (McClements, 2015). For this reason, emulsions were produced with low shear (12,000 rpm) for this aspect of the study. Moreover, EYG concentrations as low as 0.5 %wt. Could successfully prepare an emulsion; however, it may result in extreme instability (Mi et al., 2022) due to insufficient surface coverage,

potentially leading to coalescence or sedimentation. Increasing EYG concentration could reduce creaming (Ercelebi & Ibanoglu, 2010) and improve emulsion stability (Mi et al., 2022; Tian et al., 2024). By employing varying concentrations of EYG (1.5 %, 3 %, 10 %) in emulsion preparation, this study investigated the effects of EYG concentration and lyophilisation on the physical stability of the oil-in-water emulsion. Furthermore, emulsion stability significantly impacts its acceptability and storability, and backscattering techniques are suitable for online measurements of large-scale and concentrated emulsions (Tandros, 2016). The MultiScan instrument and matching software (MS 20, Dataphysics, Germany) were used to evaluate stability changes in the emulsion samples.

Furthermore, backscattering is sensitive to particle dynamics and structural changes (particle size, distribution, and aggregation). Since the primary goal of the analysis is to study the stability, the results of the backscattering profile are presented in Fig. S4 (supplementary file). The

Table 1b

Three percentiles of the droplet size distribution of emulsions produced at different EYG concentrations and shear rates.

	Non-Lyophilised (μm)	Lyophilised (µm)	Non-Lyophilised (μm)	Lyophilised (µm)	Non-Lyophilised (µm)	Lyophilised (μm)
12,000 rpm	1.5 % EYG concentration		3 % EYG concentration		10 % EYG concentration	
D10 (μm) D50 (μm) D90 (μm)	8.58 ^{hijklm} 17.17 ^{cdef} 31.82 ^b	7.83 ^{hijklm} 21.72 ^{cd} 41.67 ^a	5.81 ^{jklm} 11.11 ^{ghij} 19.19 ^{cde}	6.57 ^{ijklm} 13.13 ^{efgh} 22.98 ^c	4.79 ^{klm} 8.59 ^{hijklm} 16.92 ^{cdef}	4.29 ^{lm} 8.33 ^{hijklm} 15.66 ^{defg}
20,000 rpm						_
D10 (μm) D50 (μm) D90 (μm)	9.59 ^{hijklm} 17.17 ^{cdef} 29.29 ^b	10.61 ^{ghijk} 21.21 ^{cd} 39.89 ^a	5.81 ^{jklm} 10.35 ^{ghijkl} 17.17 ^{cdef}	7.07 ^{hijklm} 12.12 ^{fghi} 19.69 ^{cd}	4.29 ^m 7.07 ^{ijklm} 11.87 ^{fghi}	3.79 ^m 6.31 ^{ijklm} 11.11 ^{ghij}

Means that do not share a letter in the table are significantly different ($P \le 0.05$)

measured zone was between 0 mm (bottom of the glass) and 50 mm (lower concentration samples)/40 mm (high concentration samples) fill level of the vial. Each figure shows backscattering intensities against the position for the different emulsion samples.

At 0 h, the backscattering profile is high across most positions, indicating many particles that scatter light effectively, with higher EYG concentrations leading to increased values. Over 24 h, the scattered intensity decreases in lower concentration samples (1.5 % and 3 % nonlyophilised and lyophilised), reflecting particle redistribution. By 24 h, the backscattering profile is significantly lower than the initial state for $1.5\,\%$ and $3\,\%$ EYG emulsions, but relatively high in $10\,\%$ EYG emulsion. At the bottom position (0–10 mm), there is a steep rise in backscattering, indicating a high concentration of particles. In the middle position (10-40 mm), the peak shifts slightly downward and becomes less pronounced over time, indicating changes in particle sedimentation. Backscattering intensity gradually declines at the top position (above 40 mm), suggesting particles were settling. Most emulsions undergo creaming or sedimentation on standing due to gravity and the density difference between the droplets and the dispersion medium (Tandros, 2016). Additionally, a decrease in the backscattering intensity at the top position of the 1.5 % samples likely shows inadequate emulsifier concentration, leading to droplet coalescence, due to the oiling-off process (McClements, 2007). Higher concentrations lead to more dynamic particle behaviour and require longer stabilisation times. We observed smoothing of the profile in 10 % EYG emulsion, indicating increased stability compared to EYG emulsions from lower concentrations and a slightly smoother profile from the start, suggesting reduced particle mobility in the lyophilised sample compared to the non-lyophilised

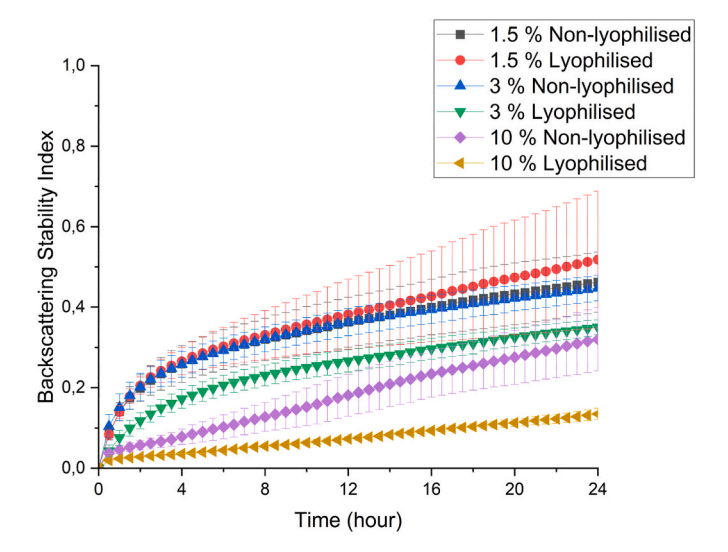


Fig. 5. Backscattering stability index of the emulsion samples against measurement time.

counterpart. The lyophilised EYG is more suitable for emulsion applications requiring immediate stability, while the non-lyophilised sample may require time to stabilise.

The ability of an emulsion to resist changes over time is known as emulsion stability (McClements, 2007). And since food emulsions could become unstable due to different physicochemical mechanisms, the backscattering signal of the emulsion samples measured over time was further analysed using the stability index (SI) function of the MS software. This computation sums all the variations detected in the sample, including sedimentation, creaming, size variation, etc. Fig. 5 quantifies the destabilisation effects of each emulsion sample over time. The average backscattering stability indices (BS-SI, %) are 0.34 \pm 0.11, 0.36 \pm 0.14, 0.34 \pm 0.10, 0.25 \pm 0.08, 0.18 \pm 0.10, and 0.07 \pm 0.04 for 1.5 % non-lyophilised, 1.5 % lyophilised, 3 % non-lyophilised, 3 % lyophilised, 10 % non-lyophilised, and 10 % lyophilised emulsion samples, respectively. The lower the BS-SI value, the more stable the sample is (Dataphysics Instruments, 2025). The BS-SI increases linearly over time for all samples, suggesting that the emulsion becomes progressively less stable as time progresses. This suggests that the samples ae undergoing destabilisation processes such as clarification, creaming, etc. The 1.5 % EYG emulsions show the fastest initial increase in the stability index, reaching a plateau earlier, while 10 % shows minimal increase even until 24 h, indicating better stability. Increasing the EYG concentration shows much lower stability indices, suggesting that higher concentration leads to greater stability. Lyophilisation promotes emulsion stabilisation, especially at higher concentration; however, at 1.5 % EYG concentration, the non-lyophilised EYG emulsion was more stable. Lyophilisation also enhances stabilisation over time compared to the non-lyophilised samples.

Results show that all the emulsion samples are relatively stable and can undergo gradual destabilisation over time. Because LDL protein is more soluble and diffuses more quickly at oil-water interfaces, nonlyophilised emulsions demonstrated higher stability at lower concentrations (1.5 & 3 % EYG). Higher concentrations are necessary for lyophilised granules to overcome their decreased solubility and disperse adequately, on the other hand. The structural integrity of the HDLphosvitin complexes which was maintained during lyophilisation, resulted in the formation of cohesive interfacial networks that provided stabilisation, so at 10 % EYG concentration, the lyophilised samples showed superior stability. This illustration supports earlier findings that a high enough concentration can lead to particles adhering to the oilwater interface and shielding individual droplets from instability (Dickinson, 2017). This provides a sufficient description of the variations in their backscattering profiles. Furthermore, all samples show increasing BS-SI over time, but the rate of change depends on the granule concentration treatment (lyophilised or non-lyophilised). As revealed in Table 2, the decrease in alteration rate after about 5 h of measurement could indicate a stabilising process, where initial rapid changes slow down over time, as the state becomes more stable. The stabilisation phase corresponds to the later period (5-24 h), where the

Table 2Backscattering stability index versus time.

Measurement time (hr)		Non-lyophilised			Lyophilised		
0-24	Alteration Rate (±) [1/h] R^2	1.5 % 0.013 (0.002) 0.854	3 % 0.012 (0.000) 0.837	10 % 0.012 (0.002) 0.994	1.5 % 0.015 (0.006) 0.871	3 % 0.011 (0.001) 0.886	10 % 0.005 (0.000) 0.993
5–24	Alteration Rate (\pm) [1/h] R^2	0.006 (0.005) 0.992	0.009 (0.000) 0.980	0.012 (0.002) 0.996	0.012 (0.006) 0.996	0.008 (0.000) 0.988	0.005 (0.001) 0.997

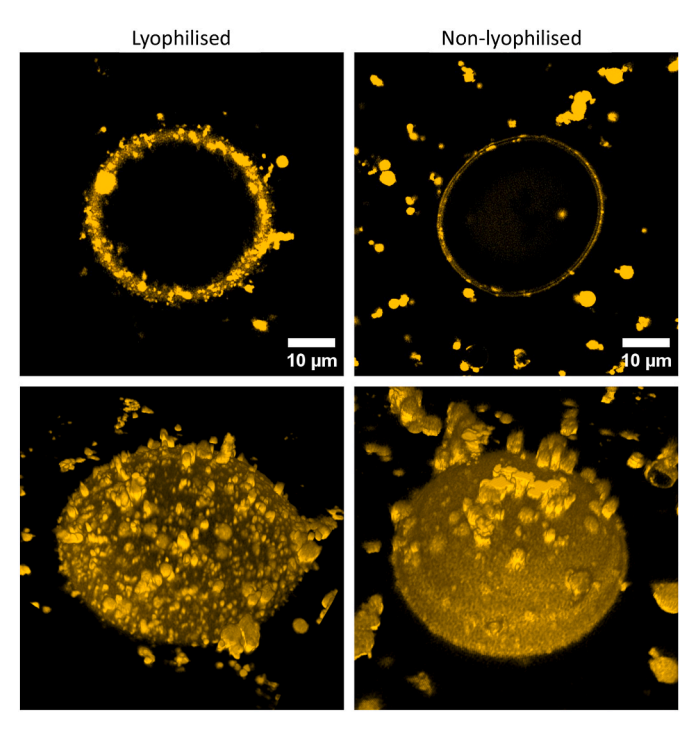


Fig. 6. Confocal Laser Scanning Microscope (CLSM) images of emulsions stabilised with 10 % lyophilised and non-lyophilised egg yolk granule (EYG).

rate of change slows down, and the higher R^2 values increase, indicating that the changes are becoming more predictable as they fit better to a linear model. Increasing the EYG concentration reduced the alteration rate per hour. The use of lyophilised EYG in the emulsion also shows a lower alteration rate per hour for all samples, indicating a more stable state, except for the 1.5 % EYG emulsion sample.

3.6. Confocal laser scanning microscope (CLSM) of the most stable emulsion samples

CLSM detected the fluorescence microstructure of the 10 % non-lyophilised and lyophilised emulsion droplets, in 2D and 3D images (Fig. 6). The 2D images revealed that the emulsion from the lyophilised EYG shows dense particle adsorption at the oil-water interface, and that of the non-lyophilised emulsion shows a thinner ring with sparser coverage. The 3D images show that the lyophilised emulsion sample formed a robust, textured shell around the droplet, indicating a stronger interfacial coverage than the non-lyophilised EYG emulsion with weaker interfacial stability since many of the particles remained in the continuous phase rather than adsorbing. These interfacial differences are consistent with molecular-level findings. DLS showed that lyophilised granules form larger, more uniform particles that are better able to form dense, cohesive interfacial layers. Furthermore, the lower zeta potential of the lyophilised EYG sample (-16.6 mV) indicates reduced electrostatic repulsion, enabling tighter packing at the droplet interface. Despite

reduced colloidal stability in dispersion, these characteristics enhance interfacial film strength and lead to improved emulsion stability. Taken together, these findings demonstrate that lyophilised EYG at a concentration of $10\,\%$ exhibits improved interfacial behaviour, resulting in the formation of the most stable emulsion.

3.7. Protein profiling of the EYG and the most stable emulsion samples

To elucidate which proteins were associated with different emulsion phases, the 10 % non-lyophilised and lyophilised emulsions were fractionated into the cream (upper), aqueous (middle), and pellet (lower) layers, and analysed by Sodium Dodecyl Sulfate Polyacrylamide Gel Electrophoresis (SDS-PAGE). The protein profiles of the whole EYG were also reported in Fig. 7.

In the cream fraction (interfacial proteins), lyophilised samples consistently exhibited more intense bands in the high molecular weight region (75–130 kDa), as well as in the Phosvitin (35–45) kDa region, than the non-lyophilised samples. In the aqueous phase, the non-lyophilised samples retained relatively higher levels of soluble proteins, particularly in the low-to-mid molecular weight (30–65 kDa) range. In the pellet fractions, the lyophilised samples contained more residual high-molecular-weight proteins, which may be due to partial aggregation or insolubility after freeze-drying. Non-lyophilised samples showed weaker pellet bands, suggesting greater solubility and dispersion of proteins. This indicates that lyophilisation alters the partitioning of EYG proteins during emulsification. Specifically, lyophilised granules deliver more HDL (lipovitellin) and phosvitin to the droplet interface, while non-lyophilised granules leave a greater proportion of proteins dispersed in the aqueous phase. This result is consistent with confocal

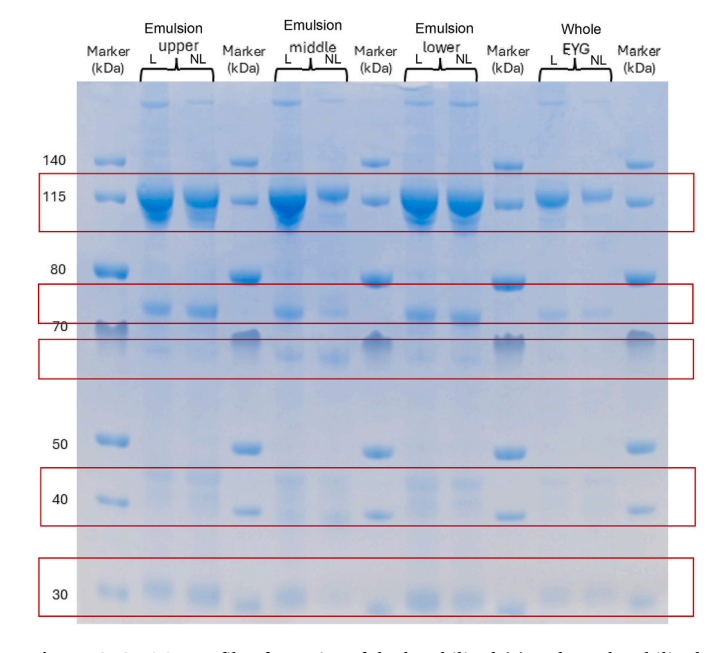


Fig. 7. SDS-PAGE profile of proteins of the lyophilised (L) and non-lyophilised (NL) whole egg yolk granule (EYG) and the 10 % EYG emulsions.

microscopy, which showed a thicker, continuous interfacial ring for lyophilised samples compared to a thinner ring with more protein in the continuous phase observed in non-lyophilised emulsions. Together, these suggest that lyophilisation promotes the exposure of HDL-phosvitin to assemble and adsorb into a particle-like interfacial structure of the EYG-based emulsion.

Protein bands identified in the samples are classified as 110 kDa (Apovitellin 3-4); 105-110 kDa (Lipovitellin, apo-HDL); 79 kDa (apo-HDL); 68 kDa (Apovitellenin IV); 47 kDa (Apovitellin 7); 45 kDa (β-phosvitin); 37 kDa (α2-phosvitin); 32 kDa (apo-HDL); 31 kDa (Apovitellin 8); 30 kDa (Lipovitellin). This is similar to those reported for EYG (Gaillard et al., 2022; Laca et al., 2014; Strixner & Kulozik, 2013). The SDS-PAGE analysis demonstrates that lyophilised EYG deposits more protein at the oil-water interface compared to non-lyophilised EYG, especially within the 75-130 kDa (lipovitellin/HDL) and 35-45 kDa (phosvitin) ranges. On the contrary, non-lyophilised samples retain more protein in the aqueous (middle) phase. This complements the confocal results, suggesting that lyophilisation reduces the presence or mobility of LDL in the interface. In addition, it drives more HDL-phosvitin to the interface, resulting in a denser interfacial layer observed in the confocal images. This corresponds to the literature that phosvitin is a potent emulsifier that stabilises interfacial film and oil-in-water emulsion, by adsorbing to the surfaces of oil droplets (Jung et al., 2013). HDL also exhibits excellent emulsifying properties, especially when soluble or paired with other compounds like phosvitin (Laca et al., 2014). In addition, although LDL are the main contributor to yolk interfacial and emulsifying properties, HDL also contributes to interfacial film formation, which is essential for stabilising emulsions (Marcet et al., 2022).

Our findings show that lyophilisation disrupts LDL and does not contribute effectively to interfacial coverage. HDL (major protein-lipid complexes with amphiphilic behaviour) undergoes structural expansion upon rehydration, and the surface hydrophobicity and emulsifying activity of phosvitin increase upon freeze-thawing (Marcet et al., 2022). This explains why increasing the concentration of the lyophilised EYG could promote greater and more cohesive deposition at the interface (thicker shell) and yield better interfacial coverage than non-lyophilised EYG.

4. Conclusions

This study highlights the structural compact of EYG after freezedrying with sharper interfaces (Porod slope >4) in contrast to salt treatment, where the granules are dissolved and their interfaces become more diffuse (Porod slope <4). The complete dissociation of LDL during freeze-drying leads to increased hydration and a larger hydrodynamic radius after rehydration. This is also reflected by a shift in the SAXS peak to lower q-values, indicating swelling of the internal HDL structure. It signifies a swelling of the remaining protein matrix, which causes the granules to appear with a more hydrated residual structure after the loss of LDL, which is retained as a stable particle.

Lyophilisation of EYG enables the granules to adsorb more effectively at the oil-water interface of emulsions and ensures uniform distribution within the continuous phase. This is probably due to the complete release of LDL and the associated exposure or rearrangement of surface-active protein components. Also, increasing the concentration of the granules further improves stabilisation by providing sufficient particles to cover the oil droplets completely. Emulsions prepared with lyophilised granules and homogenised at higher speed showed significant uniformity of droplet size and stability.

The backscattering intensities increase in the lower phase of the system due to the redistribution of particles, remain stable in the middle phase, suggesting uniform dispersion, and then decrease towards the upper phase (in $1.5\,\%$ and $3\,\%$ EYG emulsions), indicating creaming or sedimentation of oil droplets. Changes in the backscattering intensities are more pronounced in the first $5\,\%$, then are reduced minimally until

the end of the measurement period. The 10 % EYG emulsion shows higher stability compared to lower concentrations, with significant phase separation observed in the 1.5 % and 3 % samples. Lyophilisation promotes HDL-phosvitin deposition at the interface, while nonlyophilised emulsion leaves more LDL/apolipoproteins in solution. SDS-PAGE corroborates the confocal images, with higher interfacial (cream) protein in lyophilised samples and more protein remaining in the aqueous phase for non-lyophilised samples. Insights from this study could inspire further research into optimising EYG for complex emulsion systems, contributing to the growing interest in natural and functional hydrocolloids for food and non-food applications. Additionally, research outlook could also aim at investigating the interface occupancy using SANS analyses and contrast matching.

CRediT authorship contribution statement

Beatrice Mofoluwaso Oladimeji: Writing – review & editing, Writing – original draft, Visualization, Validation, Resources, Methodology, Investigation, Formal analysis, Data curation, Conceptualization. Thomas Pütz: Writing – review & editing, Visualization, Validation, Investigation, Formal analysis, Data curation, Writing – original draft. Baohu Wu: Writing – review & editing, Methodology, Investigation, Formal analysis. Theresia Heiden-Hecht: Writing – review & editing, Resources, Methodology, Formal analysis. Olaf Holderer: Writing – review & editing, Resources, Methodology. Stephan Förster: Resources, Methodology. Ronald Gebhardt: Writing – review & editing, Visualization, Validation, Supervision, Resources, Methodology, Investigation, Funding acquisition, Formal analysis, Data curation, Conceptualization, Writing – original draft.

Funding sources

This research did not receive any specific grant from funding agencies in the public, commercial, or not-for-profit sectors.

Declaration of competing interest

The authors declare that they have no known competing financial interests or personal relationships that could have appeared to influence the work reported in this paper.

Acknowledgment

We thank Ms. Milena Jerosch and Mr. Tobias Schrader (Heinz Maier-Leibnitz-Zentrum, Garching) for their support with the preparation and characterisation of the samples for SAXS. We thank Mr. Tobias Horbach (Forschungszentrum, Jülich) for his support with the SDS-PAGE analysis. We also thank Henrik Kratzer, Jérôme Jordan and Jonas Spehr for their valuable assistance in our laboratory.

Appendix A. Supplementary data

Supplementary data to this article can be found online at https://doi.org/10.1016/j.foodhyd.2025.112170.

Data availability

Data will be made available on request.

References

Abeyrathne, E. D. N. S., Nam, K.-C., Huang, X., & Ahn, D. U. (2022). Egg yolk lipids: Separation, characterization, and utilization. Food Science and Biotechnology, 31(10), 1243–1256. https://doi.org/10.1007/s10068-022-01138-4

Alcay, S., Gokce, E., Toker, M. B., Onder, N. T., Ustuner, B., Uzabacı, E., Gul, Z., & Cavus, S. (2016). Freeze-dried egg yolk based extenders containing various antioxidants improve post-thawing quality and incubation resilience of goat

- spermatozoa. Cryobiology, 72(3), 269–273. https://doi.org/10.1016/j.
- Anthuparambil, N. D., Girelli, A., Timmermann, S., Kowalski, M., Akhundzadeh, M. S., Retzbach, S., Senft, M. D., Dargasz, M., Gutmüller, D., Hiremath, A., Moron, M., Öztürk, Ö., Poggemann, H.-F., Ragulskaya, A., Begam, N., Tosson, A., Paulus, M., Westermeier, F., Zhang, F., ... Gutt, C. (2023). Exploring non-equilibrium processes and spatio-temporal scaling laws in heated egg yolk using coherent X-rays. Nature Communications, 14(1), 5580. https://doi.org/10.1038/s41467-023-41202-z
- Anthuparambil, N. D., Timmermann, S., Dargasz, M., Retzbach, S., Senft, M. D., Begam, N., Ragulskaya, A., Paulus, M., Zhang, F., Westermeier, F., Sprung, M., Schreiber, F., & Gutt, C. (2024). Salt induced slowdown of kinetics and dynamics during thermal gelation of egg-yolk. *The Journal of Chemical Physics*, 161(5), Article 055102. https://doi.org/10.1063/5.0219004
- Bhosale, S., Kumbhar, P., Patil, O., Landage, K., Kabade, R., Manjappa, A., & Disouza, J. (2021). Lyophilization: Principle, methods, and applications. *Drug and Pharmaceutical Science Archives*, 1(1), 10–14.
- Bie, J., Cao, J., Peng, Z., Wang, J., Wang, Y., Zhang, Y., Ding, Y., & Teng, W. (2025). Studies on the complex interactions of different egg yolk proteins and their roles on rheological properties and stability of high internal phase pickering emulsions. *Food Hydrocolloids*, 160, Article 110755. https://doi.org/10.1016/j.
- Chen, Y., Chen, Y., Jiang, L., Yang, Z., Fang, Y., & Zhang, W. (2023). Shear emulsification condition strategy impact high internal phase pickering emulsions stabilized by coconut globulin-tannic acid: Structure of protein at the oil-water interface. Lebensmittel-Wissenschaft und -Technologie, 187, Article 115283. https://doi.org/10.1016/j.lwt.2023.115283
- Ciurzyńska, A., & Lenart, A. (2011). Freeze-Drying—Application in food processing and biotechnology—A review. Polish Journal of Food and Nutrition Sciences, 61(3), 165–171. https://doi.org/10.2478/v10222-011-0017-5
- Danaei, M., Dehghankhold, M., Ataei, S., Hasanzadeh Davarani, F., Javanmard, R., Dokhani, A., Khorasani, S., & Mozafari, M. R. (2018). Impact of particle size and polydispersity index on the clinical applications of lipidic nanocarrier systems. *Pharmaceutics*, 10(2), 57. https://doi.org/10.3390/pharmaceutics10020057
- Dataphysics Instruments. (2025). Stability Analysis of Milk-like Products -To study the destabilisation mechanism in different milk substitutes [Application Notes]. https://www.dataphysics-instruments.com/application/notes/.
- Dickinson, E. (2017). Biopolymer-based particles as stabilizing agents for emulsions and foams. Food Hydrocolloids, 68, 219–231. https://doi.org/10.1016/j. foodhyd.2016.06.024
- Ercelebi, E. A., & Ibanoglu, E. (2010). Stability and rheological properties of egg yolk granule stabilized emulsions with pectin and guar gum. *International Journal of Food Properties*, 13(3), 618–630. https://doi.org/10.1080/10942910902716984
- Fernandez-Moure, J., Maisha, N., Lavik, E. B., & Cannon, J. W. (2018). The chemistry of lyophilized blood products. *Bioconjugate Chemistry*, 29(7), 2150–2160. https://doi. org/10.1021/acs.bioconichem.8b00271
- Gaillard, R., Marciniak, A., Brisson, G., Perreault, V., House, J. D., Pouliot, Y., & Doyen, A. (2022). Impact of ultra-high pressure homogenization on the structural properties of egg Yolk Granule. *Foods*, 11(4). https://doi.org/10.3390/foods11040512. Article 4.
- Gatto, M. S., & Najahi-Missaoui, W. (2023). Lyophilization of nanoparticles, does it really work? Overview of the Current status and challenges. *International Journal of Molecular Sciences*, 24(18). https://doi.org/10.3390/ijms241814041. Article 18.
- Gerony, F., Fanost, A., Tan, Z. R., Malikova, N., Michot, L., Poirier-Quinot, M., Viguerie, L. de, Jaber, M., Mériguet, G., & Rollet, A.-L. (2025). Structural and dynamical impacts of water dilution on egg yolk properties. *Soft Matter*, 21(23), 4666–4680. https://doi.org/10.1039/D5SM00289C
- Gmach, O., Golda, J., & Kulozik, U. (2022). Freeze-thaw stability of emulsions made with native and enzymatically modified egg yolk fractions. *Food Hydrocolloids, 123*, Article 107109. https://doi.org/10.1016/j.foodhyd.2021.107109
- Heiden-Hecht, T., Wu, B., Schwärzer, K., Förster, S., Kohlbrecher, J., Holderer, O., & Frielinghaus, H. (2024). New insights into protein stabilized emulsions captured via neutron and X-ray scattering: An approach with β-lactoglobulin at triacylglycerideoil/water interfaces. *Journal of Colloid and Interface Science*, 655, 319–326. https://doi.org/10.1016/j.jcis.2023.10.155
- Hu, G., Liu, X., Wu, D., Wang, B., Wang, J., & Geng, F. (2023). Quantitative N-glycoproteomic analysis of egg yolk powder during thermal processing. Food Research International, 174, Article 113678. https://doi.org/10.1016/j.foodres.2023.113678
- Jung, S., Ahn, D. U., Nam, K. C., Kim, H. J., & Jo, C. (2013). Separation of Phosvitin from egg yolk without using organic solvents. Asian-Australasian Journal of Animal Sciences, 26(11), 1622–1629. https://doi.org/10.5713/ajas.2013.13263
- Khan, M. M., Sun, S., Shi, R., Aichun, L., Lee, O.-H., & Fu, X. (2025). Biodegradable and antibacterial edible films based on egg yolk granules/gelatin/CMC with e-poly-llysine: Application in fresh chicken meat preservation. *Food Chemistry*, 478, Article 143627. https://doi.org/10.1016/j.foodchem.2025.143627
- Laca, A., Paredes, B., & Díaz, M. (2010). A method of egg yolk fractionation. Characterization of fractions. Food Hydrocolloids, 24(4), 434–443. https://doi.org/10.1016/j.foodhyd.2009.11.010
- Laca, A., Paredes, B., Rendueles, M., & Díaz, M. (2014). Egg yolk granules: Separation, characteristics and applications in food industry. LWT Food Science and Technology, 59(1), 1–5. https://doi.org/10.1016/j.lwt.2014.05.020
- Li, Q., Tang, S., Mourad, F. K., Zou, W., Lu, L., & Cai, Z. (2020). Emulsifying stability of enzymatically hydrolyzed egg yolk granules and structural analysis. *Food Hydrocolloids*, 101, Article 105521. https://doi.org/10.1016/j. foodhyd.2019.105521

- Li, X., Wang, Y.-M., Sun, C.-F., Lv, J.-H., & Yang, Y.-J. (2021). Comparative Study on foaming properties of egg white with yolk fractions and their hydrolysates. *Foods*, 10 (9). https://doi.org/10.3390/foods10092238. Article 9.
- Liu, J., Wang, Y., Zou, Y., Wu, Y., Guan, W., Yang, J., & Li, X. (2024). Foaming and structural properties of egg yolk components microgel particles and their adsorption characteristics at the air-water interface. Food Hydrocolloids, 152, Article 109842. https://doi.org/10.1016/j.foodhyd.2024.109842
- Malvern, P. (2010). Zeta Potential Measurement of Highly Concentrated CMP Slurry Dispersions [Application Notes]. https://www.malvernpanalytical.com/en/learn/k nowledge-center/application-notes/an101104highlyconcentratedcmpslurry.
- Marcet, I., Sáez-Orviz, S., Rendueles, M., & Díaz, M. (2022). Egg yolk granules and phosvitin. Recent advances in food technology and applications. *Lebensmittel-Wissenschaft und -Technologie*, 153, Article 112442. https://doi.org/10.1016/j. lwt.2021.112442
- McClements, D. J. (2004). 7. Emulsion stability. In Food Emulsions: Principles, practices, and techniques (2nd ed., pp. 319–325). CRC Press.
- McClements, D. J. (2007). Critical review of techniques and methodologies for characterization of emulsion stability. Critical Reviews in Food Science and Nutrition, 47(7), 611–649. https://doi.org/10.1080/10408390701289292
- McClements, D. J. (2015). Emulsion stability. In Food emulsions: Principles, practices, and techniques (3rd ed., p. 94). CRC Press.
- Mi, S., Xia, M., Zhang, X., Liu, J., & Cai, Z. (2022). Formation of natural egg Yolk Granule stabilized pickering high internal phase emulsions by means of NaCl ionic strength and pH change. Foods, 11(2). https://doi.org/10.3390/foods11020229. Article 2.
- Motta-Romero, H., Zhang, Z., Tien Nguyen, A., Schlegel, V., & Zhang, Y. (2017). Isolation of Egg Yolk Granules as Low-Cholesterol Emulsifying Agent in Mayonnaise: Egg yolk granules as low-cholesterol emulsifier. *Journal of Food Science*, 82(7), 1588–1593. https://doi.org/10.1111/1750-3841.13747
- Naderi, N., Pouliot, Y., House, J. D., & Doyen, A. (2017). Effect of freezing, thermal pasteurization, and hydrostatic pressure on fractionation and folate recovery in egg yolk. *Journal of Agricultural and Food Chemistry*, 65(35), 7774–7780. https://doi.org/ 10.1021/acs.jafc.7b02892
- Oka, Y., Yukawa, H., Kudo, H., Ooka, K., Wada, M., Suetaka, S., Chang, M., Kawai, H., Tanaka, R., Ichikawa, M., Suzuki, T., Hayashi, Y., Handa, A., & Arai, M. (2022). A comparative study of unpasteurized and pasteurized frozen whole hen eggs using size-exclusion chromatography and small-angle X-ray scattering. *Scientific Reports*, 12(1), 9218. https://doi.org/10.1038/s41598-022-12885-z
- Oladimeji, B. M., & Gebhardt, R. (2023). Physical characteristics of egg yolk granules and effect on their functionality. Foods, 12(13). https://doi.org/10.3390/ foods12132531. Article 13.
- Shen, Y., Chang, C., Shi, M., Su, Y., Luping, G., Li, J., & Yang, Y. (2019). Interactions between lecithin and yolk granule and their influence on the emulsifying properties. *Food Hydrocolloids*, 101, Article 105510. https://doi.org/10.1016/j. foodhyd.2019.105510
- Soraiyay Zafar, H., Asefi, N., Siahpoush, V., Roufegarinejad, L., & Alizadeh, A. (2023). Preparation of egg white powder using electrohydrodynamic drying method and its effect on quality characteristics and functional properties. Food Chemistry, 426, Article 136567. https://doi.org/10.1016/j.foodchem.2023.136567
- Strixner, T., & Kulozik, U. (2013). Continuous centrifugal fractionation of egg yolk granules and plasma constituents influenced by process conditions and product characteristics. *Journal of Food Engineering*, 117(1), 89–98. https://doi.org/10.1016/j.ifoodeng.2013.02.009
- Strixner, T., Sterr, J., Kulozik, U., & Gebhardt, R. (2014). Structural Study on Hen-egg Yolk High Density Lipoprotein (HDL) granules. Food Biophysics, 9(4), 314–321. https://doi.org/10.1007/s11483-014-9359-y
- Suhag, R. (2024). Egg yolk, a multifunctional emulsifier: New insights on factors influencing and mechanistic pathways in egg yolk emulsification. *Applied Sciences*, 14(21), 9692. https://doi.org/10.3390/app14219692
- Sztorch, B., Nowak, K., Frydrych, M., Leśniewska, J., Krysiak, K., Przekop, R. E., & Olejnik, A. (2023). Improving the dispersibility of TiO2 in the colloidal System using trifunctional spherosilicates. *Materials*, 16(4), 1442. https://doi.org/10.3390/mps16041442
- Tandros, T. F. (2016). 13. Characterization of emulsions and assessment of their stability. In *Emulsions: Formation, stability, industrial applications* (pp. 173–196). De Gruyter. https://doi.org/10.1515/9783110452242-014.
- Thierau, S., Keil, H., Seuss-Baum, I., & Hensel, O. (2014). Effects of heat treatment and freeze-drying on the protein and lipoprotein structures of egg yolk as determined using Differential Scanning Calorimetry (DSC). Agricultural Communications, 2(3), 27, 27
- Tian, Y., Lv, X., Oh, D.-H., Kassem, J. M., Salama, M., & Fu, X. (2024). Emulsifying properties of egg proteins: Influencing factors, modification techniques, and applications. Comprehensive Reviews in Food Science and Food Safety, 23(5), Article e70004. https://doi.org/10.1111/1541-4337.70004
- Vargas-del-Río, L. M., García-Figueroa, A., Fernández-Quintero, A., & Rodríguez-Stouvenel, A. (2022). Spray-Drying hen eggs: Effects of the egg yolk to egg white ratio and sucrose addition on the physicochemical, functional, and nutritional properties of dried products and on their amino acid profiles. Applied Sciences, 12(9), 4516. https://doi.org/10.3390/app12094516
- Wang, A., Xiao, Z., Wang, J., Li, G., & Wang, L. (2020). Fabrication and characterization of emulsion stabilized by table egg-yolk granules at different pH levels. *Journal of the Science of Food and Agriculture*, 100(4), 1470–1478. https://doi.org/10.1002/ jsfa.10154
- Ye, H., Sui, J., Wang, J., Wang, Y., Wu, D., Wang, B., & Geng, F. (2023). Research Note: Aggregation-depolymerization of chicken egg yolk granule under different food

- processing conditions. *Poultry Science*, 102(7), Article 102696. https://doi.org/10.1016/j.psj.2023.102696
- Zanatta, V., Rezzadori, K., Penha, F. M., Zin, G., Lemos-Senna, E., Petrus, J. C. C., & Di Luccio, M. (2017). Stability of oil-in-water emulsions produced by membrane emulsification with microporous ceramic membranes. *Journal of Food Engineering*, 195, 73–84. https://doi.org/10.1016/j.jfoodeng.2016.09.025
- Zhang, Y., Xie, Y., Qiu, M., He, H., Liao, D., Zhao, H., Hu, G., & Geng, F. (2025). Insight into the difference in nutritional yolk granules of different poultry eggs from the perspective of quantitative lipidomics combined with nutrient analysis. *Food Science and Human Wellness*. https://doi.org/10.26599/FSHW.2025.9250532